

P2.18 Recent trend of Hadley and Walker circulation shown in water vapor transport potential

Seong-Chan Park and *Byung-Ju Sohn

School of Earth and Environmental Sciences
Seoul National University, Seoul, Korea

1. Introduction

In recent years, there are many studies focusing on satellite observations of long-term changes in tropical cloud and radiation [Chen *et al.*, 2002; Wielicki *et al.*, 2002; Allan and Slingo 2002; Wang *et al.*, 2002]. The analysis of satellite-based outgoing longwave radiation (OLR) at the top of the atmosphere (TOA) over the period 1985-2000 suggested that there has been an increase in the tropical mean OLR at TOA [Wielicki *et al.*, 2002]. In addition, Chen *et al.* [2002] argued that changes in radiation budget are due to an increase in the strength of the Hadley circulation.

Attentions were given to the long-term variability of the Hadley and Walker circulations using the various reanalysis data [Oort and Yienger, 1996; Trenberth *et al.*, 2000; Wang, 2002]. Mitas and Clement [2005] suggested that the NCEP and ERA40 appear to be in agreement with the strengthening of the Hadley circulation in recent decades, and Tanaka *et al.* [2004] also indicated the strengthened trend of Hadley circulation by using the maximum velocity potential of the upper troposphere obtained from NCEP reanalysis data.

On the other hand, it is suggested that there has already been a weakening of the Walker circulation in the past century, and that the observed changes are consistent with those expected as a response to increases in anthropogenic greenhouse gases [Vecchi *et al.*, 2006].

Although these previous studies have provided useful information of interannual variations of Hadley and Walker circulations, some questions should be explored: (1) How are the recent trend of Hadley and Walker circulation associated with the hydrological cycle from satellite observations and the global reanalysis data? (2) Are these trends robust among satellite and reanalysis data? To address these questions, we examine the interannual variation of Hadley and Walker circulation by using satellite measurements together with various reanalysis data in association with hydrological cycle.

2. Methodology and datasets

The methodology used here for deriving water vapor transports over the global oceans from satellite-retrieved precipitation (P) and evaporation (E) is described in detail in Sohn *et al.* [2004] and Park *et al.* [2007]. Briefly, for a given atmospheric column, the water balance is achieved as follows:

$$\frac{\partial W}{\partial t} + \nabla \cdot \mathbf{Q} = E - P, \quad (1)$$

where W is the total amount of precipitable water, E and P are evaporation and precipitation, respectively. \mathbf{Q} is the horizontal water vapor transport vector defined by

$$\mathbf{Q} = \frac{1}{g} \int_{p_0}^{p_s} q \mathbf{V} dp, \quad (2)$$

where g is the acceleration of gravity, q is specific humidity, \mathbf{V} is the horizontal wind vector, p_s is the pressure at the surface, and p_0 is the pressure at the top of the atmosphere.

In the case of satellite measurements, the Special Sensor Microwave Imager (SSM/I) onboard the Defense Meteorological Satellite Program (DMSP) satellite, by separating the water vapor transport vector (\mathbf{Q}) into rotational (\mathbf{Q}_R) and divergent (\mathbf{Q}_D) components [Chen, 1985; Sohn *et al.*, 2004]

*Corresponding author's address

Prof. Byung-Ju Sohn
School of Earth and Environmental Sciences
Seoul National University, NS80
Seoul, 151-747, Korea
E-mail: sohn@snu.ac.kr
Phone:+82-2-880-7783, Fax:+82-2-872-8156

and introducing the water vapor transport potential function (Φ) we effectively remove the rotational component (\mathbf{Q}_R), i.e.:

$$\nabla \cdot \mathbf{Q}_D = E - P - \frac{\partial W}{\partial t} = -\nabla^2 \Phi \quad (3)$$

$$\mathbf{Q}_D = -\nabla \Phi \quad (4)$$

Equations (3) and (4) are solved for Φ by using a spectral method on a global domain with inputs of evaporation, precipitation, and total precipitable water.

In the reanalyses, however, water vapor transports are directly calculated from q and \mathbf{V} data for more realistic depiction of water vapor transport rather than indirectly calculated from the $E-P$ field. It is because q and \mathbf{V} fields are produced by assimilating the model outputs to various observations. In doing so, vertically integrated water vapor transport vectors (\mathbf{Q}) are obtained by applying Eq. (2) to reanalysis data, and then a similar methodology used for the SSM/I calculation is applied for calculating the potential function, i.e.:

$$\nabla \cdot \mathbf{Q} = -\nabla^2 \Phi \quad (5)$$

The same spherical harmonics approach is employed to avoid the boundary value problems for solving potential functions. The associated divergent component of water vapor transport (\mathbf{Q}_D) in the reanalyses is then obtained by taking the gradient of potential function as in Eq. (4).

In this study, we used the simple separation of the tropical circulations proposed by *Tanaka et al.*, [2004] to define the Hadley and Walker circulations. The water vapor transport potential function (Φ) is separated into the following linear combinations of spatial patterns:

$$\begin{aligned} \Phi(t, x, y) &= [\Phi(t, y)] + \Phi^*(t, x, y) \\ &= [\Phi(t, y)] + \bar{\Phi}^*(x, y) + \Phi^*(t, x, y) \end{aligned} \quad (6)$$

where x , y , and t are longitude, latitude, and time. $[\]$ and $()^*$ represent the zonal mean and the deviation from the zonal mean, respectively. Also denoted are $()$ and $()^*$ the annual mean and the deviation from the annual mean, respectively. From Eq. (6), the Hadley circulation is defined by zonal mean field of (Φ), i.e., $[\Phi(t, y)]$ by assuming that

the Hadley circulation is an axisymmetric part of the circulation. The monsoon circulation is considered as a part of the seasonal change of the deviation field. Thus, the seasonal mean is subtracted from the deviation field to define the interannual variation of the monsoon circulation, i.e., $\Phi^*(t, x, y)$. Finally, the Walker circulation is defined by the annual mean of the zonal deviation field, i.e., $\bar{\Phi}^*(x, y)$.

The SSM/I-derived precipitation and total precipitable water [*Wentz and Spencer* 1998] for the May-September period of the years from 1988 to 2000 were obtained (from <http://www.ssmi.com>). The evaporation data were obtained from the products based upon an algorithm developed by *Chou* [1993].

The used datasets for specific humidity (q), and horizontal wind fields (\mathbf{V}) were obtained from following three reanalysis products:

- NCEP/NCAR reanalysis (NCEP, 1979-2006 [*Kalnay et al.*, 1996])
- ECMWF 40-year reanalysis (ERA40, 1979-2001 [*Simmons and Gibson*, 2000])
- Japanese 25-year reanalysis (JRA25, 1979-2004 [*Onogi et al.*, 2005])

3. Interannual variability of the Hadley and Walker circulation

3.1 Derived water vapor transport and zonal mean of potential function

Using the definition of Hadley and Walker circulation index as described in Eq. (6), we first examine the characteristics of seasonal change of the Hadley circulation. Figure 1 presents the spatial pattern of derived water vapor transport (left panels) and the zonal mean of water vapor transport potential function (Φ) (right panels) from ERA40 for the climate (1979-2001). During the DJF period (Figure 1a), the divergent water vapor is transported from the positive peak of Φ over the subtropical northwestern Pacific to the minimum of it over the western Pacific warm pool region. The zonal mean of Φ is positive in the Northern Hemisphere (NH) with a peak at 25°N. The gradient of Φ over the subtropics in the NH yields the divergent component of water vapor transport so that the water vapor is transported toward both north and south of 25°N where moisture divergence is formed. On the other hand, the

local saddle point of Φ is located near 5°N so that moisture convergence is formed by moisture transports from the NH. The pronounced meridional convergent flow over the equator represents the lower branch of the Hadley circulation in the boreal winter.

In the JJA mean climatology (Figure 1b), strong divergent water vapor transport from the SH to the NH is found over the Asian monsoon region. The zonal mean of Φ is negative in the NH and positive in the SH. The meridional water vapor transport is thus obviously stronger than that in the boreal winter. The zonal mean of Φ is positive in the SH with a local maximum at about 35°S where the moisture divergence is established. On the other hand, the local saddle point of (Φ) is located near the ITCZ where moisture convergence is formed by moisture transports from the SH. The strong water vapor is thus transported from the SH to the NH, indicating the overturning of the Hadley cell over the equator during the boreal summer.

Since the intensity of water vapor transport is determined by the gradient of its potential function, the Hadley circulation index is defined here by using the difference between positive and negative peaks of the zonal mean water vapor transport potential function. A stronger Hadley circulation can be expected when the difference in potential function at those two points is larger.

On the other hand, for separating the Walker circulation from the divergent circulation, we construct the deviation field from the zonal mean water vapor transport potential function representing the Hadley circulation, and then take its annual mean as described in Eq. (6). Figure 1c shows the annual mean of the zonal deviation field of water vapor transport potential function and associated moisture transports from ERA40. The wavenumber one pattern of Φ over the tropical Pacific Ocean indicates the feature of the Walker circulation with the moisture convergence center at the equatorial western Pacific and the moisture divergence at the eastern Pacific, resulting in westward water vapor transports from the eastern Pacific to the western Pacific. Another moisture divergence is found over the Atlantic Ocean.

With reference to Hadley circulation index, the intensity of the Walker circulation

is measured by the difference of area-averaged water vapor transport potential function shown in Figure 1c between the tropical western Pacific (10°S – 10°N , 80°E – 160°E) and the tropical eastern Pacific (10°S – 10°N , 160°W – 80°W). Based on the definition of Hadley and Walker circulation indices, the interannual variation of the intensity of the Hadley and Walker circulation from satellite and reanalyses is given in the following section.

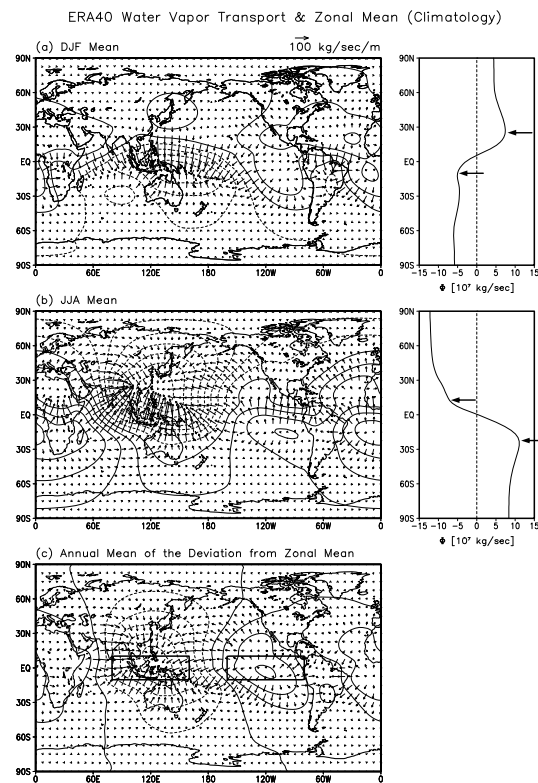


Figure 1: Long-term mean water vapor transport [Q_D] (arrow) and potential function [Φ] (contour) in (a) DJF, (b) JJA, and (c) annual mean of the deviation from zonal mean in ERA40 for the period 1979-2001. Solid rectangles in (c) indicate the regions used to define the Walker circulation index. The contour intervals of [Φ] are $5.0 \times 10^7 \text{ kg s}^{-1}$. The zonal mean potential function used to define the Hadley circulation index is shown in the panels on the right-hand side.

3.2 Hadley circulation index

Figure 2 presents the time series of the Hadley circulation index in DJF and JJA calculated from SSM/I, NCEP, ERA40, and JRA25. For DJF, there is an increasing trend in the intensity of the Hadley circulation from all datasets (Figure 2a). The intensities in ERA40 are similar to those in SSM/I from 1988 to 2000 and stronger than NCEP and JRA25 reanalyses. It is noted that there are maximum intensities related to the strongest El Niño events in 1982/83 and 1997/98 in ERA40. Intensities in NCEP and JRA25 are comparable to each other with the same phase of El Niño events shown in ERA40. This result is consistent with the previous studies [Oort and Yienger, 1996; Quan *et al.*, 2004], showing that there exist significant correlations between the Hadley circulation and the ENSO phenomenon. Mitas and Clement [2005] also found a significant intensification of the Hadley circulation from both NCEP and ERA40 by examining DJF mean stream function of the mean meridional circulation.

For JJA (Figure 2b), however, there is no clear trend in NCEP and JRA25 while there are increasing trends in SSM/I and ERA40. It is also of interest to note that there are peak intensities related to El Niño events even though peak intensities are not clearer than those in DJF. One of the possible explanations for the difference of trend of Hadley circulation between the boreal winter and summer is that the intensity of Hadley circulation is closely related to the El Niño events which become stronger during the boreal winter.

3.3 Walker circulation index

The timeseries of the Walker circulation index defined by the difference of area-averaged water vapor transport potential function as shown in Figure 1c is presented in Figure 3, along with the Niño 3.4 index. We first compared the Walker circulation index with the Niño 3.4 index, considering whether the Walker circulation index is consistent with the associated ENSO events. Generally high correlations (~ 0.80) are found in the SSM/I and reanalyses although the analysis period in SSM/I is relatively shorter than those in the other reanalyses. The highest correlation of 0.84 is found in NCEP followed by the

correlations of 0.82, 0.08, and 0.79 in JRA25, SSM/I, and ERA40, respectively.

In the case of SSM/I (Figure 3a), there is a weakening trend of the Walker circulation with two noticeable El Niño events in 1991/92 and 1997/98 because of no satellite records before 1988 in SSM/I. The NCEP and ERA40 also show a weakening trend of the Walker circulation in recent decades with El Niño events in 1982/83, 1986/87, 1991/92, 1994/95, and 1997/98 (Figures 3b-c) whereas there is no clear weakening trend of the Walker circulation in JRA25 although it captures associated ENSO events (Figure 3d). This weakening trend of Walker circulation in this study is consistent with the previous studies [Vecchi *et al.*, 2006; Zhang and Song, 2006] in which the sea-level pressure differences between the western and eastern Pacific are used for the Walker circulation index. This result is also consistent with the Walker circulation index defined by Wang [2002] using the difference of 500 hPa vertical velocities between the eastern and the western Pacific. Since the weaker Walker circulation is accompanied by the El Niño-like SST pattern, the result in recent decades is consistent with the recent trend of the enhanced El Niño-like SST pattern [IPCC, 2001].

4. Conclusion

In this paper, we examined the trend of Hadley and Walker circulation by using satellite measurements from SSM/I together with NCEP, ERA40, and JRA25 reanalysis data in association with hydrological cycle.

The time series of the Hadley circulation index indicates intensifying trend in boreal winter from SSM/I and all three reanalyses. However, there is no clear trend in all reanalyses while there is an increasing trend from SSM/I in boreal summer. On the other hand, the Walker circulation index shows a weakening trend in recent decades in SSM/I and all three reanalyses. These trends of Hadley and Walker circulations are consistent with the previous studies [Oort and Yienger, 1996; Quan *et al.*, 2004; Vecchi *et al.*, 2006; Zhang and Song, 2006], although in which are applied different method to definition of Hadley and Walker circulation indices.

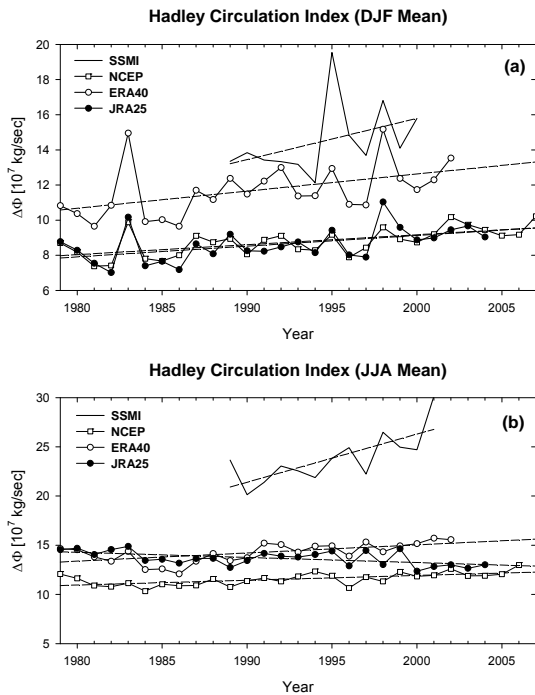


Figure 2: The timeseries of the Hadley circulation index defined by the difference of zonal mean potential function between its peaks in the Southern Hemisphere and Northern Hemisphere in (a) DJF and in (b) JJA.

In summary, there appears to be agreement that the Hadley circulation during the northern hemispheric winter has been intensified over the past decades among SSM/I, NCEP, ERA40, and JRA25, related to the El Niño's interannual fluctuations including larger amplitude and increased frequency after 1976 [Quan *et al.*, 2004]. The Walker circulation, then, appears to be weakening along with the intensification in the El Niño. Although the trends of Hadley and Walker circulations are not consistent with all of datasets, it can be suggested that the changes of Hadley and Walker circulation intensities are evident from the results of satellite and reanalysis data.

Changes in Hadley and Walker circulation may be caused by changes of various climatic parameters such as cloud, water vapor, and aerosol, and their complicated interactions. Thus, it is important to investigate and understand the characteristics of climatic variables, in particular, in recent climate change studies. Accurate and continuous satellite

observations of radiation, water budget variables, and aerosol distribution can provide one possibility of addressing inconsistencies between satellite and reanalysis data by comparing the observed and simulated changes in the atmospheric circulation associated with the hydrological cycle.

Acknowledgements

This research has been supported by the SRC program of the Korea Science and Engineering Foundation, and also by the BK21 Project of the Korean Government.

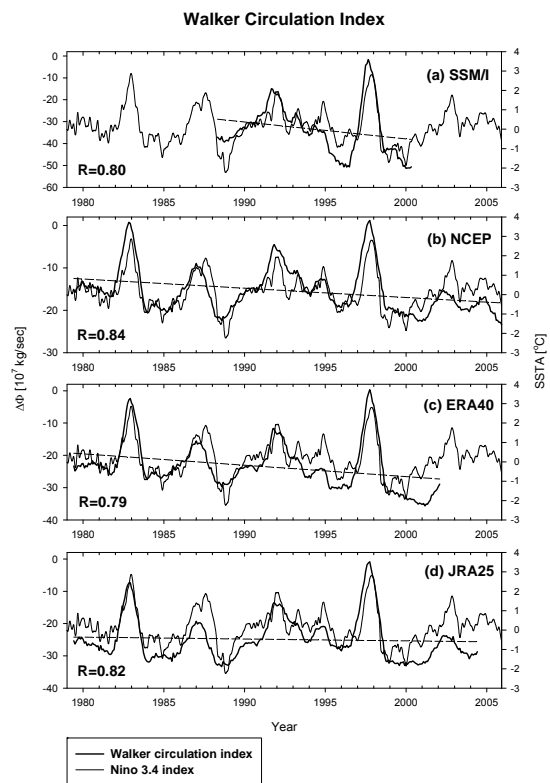


Figure 3: The timeseries of the Walker circulation index (thick lines) from (a) SSM/I, (b) NCEP, (c) ERA40, and (d) JRA25, along with the Niño 3.4 SST index (thin lines). The Walker circulation index is defined by the difference of area-averaged potential function between the tropical western Pacific (10°S–10°N, 80°E–160°E) and the tropical eastern Pacific (10°S–10°N, 160°W–80°W).

References

- Allan, R. P., and A. Slingo, 2002: Can current climate model forcings explain the spatial and temporal signatures of decadal OLR variations? *Geophys. Res. Lett.*, **29**, doi: 10.1029/2001GL014620.
- Chen, J., B. E. Carlson, and A. D. Del Genio, 2002: Evidence for strengthening of the tropical general circulation in the 1990s. *Science*, **295**, 838-841.
- Chen, T. C., 1985: Global water vapor flux and maintenance during FGGE. *Mon. Wea. Rev.*, **113**, 1801-1919.
- Chou, S. H., 1993: A comparison of airborne eddy correlation and bulk aerodynamic methods for ocean-air turbulent fluxes during cold-air outbreaks. *Bound.-Layer Meteor.*, **64**, 75-100.
- IPCC, 2001: *Climate change 2001: The Scientific Basis*, edited by Houghton, J. T., Y. Ding, D. J. Griggs, M. Noguer, P. J. van der Linden, X. Dai, K. Maskell, and C. A. Johnson, Cambridge University Press, 881pp.
- Kalnay, E., and Coauthors, 1996: The NCEP/NCAR 40-year reanalysis project. *Bull. Amer. Meteor. Soc.*, **77**, 437-471.
- Mitas, C. M. and A. Clement, 2005: Has the Hadley cell been strengthening in recent decades? *Geophys. Res. Lett.*, **32**, doi: 10.1029/2004GL021765.
- Onogi, K., H. Koide, M. Sakamoto, S. Kobayashi, J. Tsutsui, H. Hatsushika, T. Matsumoto, N. Yamazaki, H. Kamahori, K. Takahshi, K. Kato, T. Ose, S. Kadokura, and K. Wada, 2005: JRA-25: Japanese 25-year re-analysis project-progress and status. *Quart. J. Roy. Meteor. Soc.*, **131**, 3259-3268.
- Oort, A. H. and J. J. Yienger, 1996: Observed interannual variability in the Hadley circulation and its connection to ENSO. *J. Clim.*, **9**, 2751-2767.
- Park, S. C., B. J. Sohn, and B. Wang, 2007: Satellite assessment of divergent water vapor transport from NCEP, ERA40, and JRA25 reanalyses over the Asian summer monsoon region. *J. Meteor. Soc. Japan*, **85**, 615-632.
- Quan, X. -W., H. F. Diaz, and M. P. Hoerling, 2004: Change in the tropical Hadley cell since 1950, in *The Hadley Circulation: Present, Past, and Future*, edited by H. F. Diaz, and R. S. Bradley, 85-120, Cambridge Univ. Press, New York.
- Simmons, A. J., and J. K. Gibson, 2000: The ERA-40 project plan, ERA-40 Project Report Series No. 1, ECMWF, Reading, UK, 62pp.
- Sohn, B. J., E. A. Smith, F. R. Robertson, and S. C. Park, 2004: Derived over-ocean water vapor transports from satellite-retrieved E-P datasets. *J. Clim.*, **17**, 1352-1365.
- Tanaka, H. L., N. Ishizaki, and A. Kitoh, 2004: Trend and interannual variability of Walker, monsoon and Hadley circulations defined by velocity potential in the upper troposphere. *Tellus*, **56A**, 250-269.
- Trenberth, K. E., D. P. Stepaniak, and J. M. Caron, 2000: The global monsoon as seen through the divergent atmospheric circulation. *J. Clim.*, **13**, 3969-3993.
- Vecchi, G. A., B. J. Soden, A. T. Wittenberg, I. M. Held, A. Leetmaa, and M. J. Harrison, 2006: Weakening of tropical Pacific atmospheric circulation due to anthropogenic forcing. *Nature*, **441**, 73-76.
- Wang, C., 2002: Atmospheric circulation cells associated with the El Nino-Southern Oscillation. *J. Clim.*, **15**, 399-419.
- Wang, P. H., P. Minnis, B. A. Wielicki, T. Wong, and L. B. Vann, 2002: Satellite observations of long-term changes in tropical cloud and outgoing longwave radiation from 1985 to 1998. *Geophys. Res. Lett.*, **29**, 10.1029/2001GL014264.
- Wentz, F. J., and R.W. Spencer, 1998: SSM/I rain retrievals within a unified all-weather ocean algorithm. *J. Atmos. Sci.*, **55**, 1613-1627.
- Wielicki, B. A., T. Wong, R. P. Allen, A. Slingo, J. T. Kiehl, B. J. Soden, C. T. Gordon, A. J. Miller, S. K. Yang, D. A. Randall, F. Robertson, J. Susskind, and H. Jacobowitz, 2002: Evidence for large decadal variability in the tropical mean radiative energy budget. *Science*, **295**, 841-844.
- Zhang, M., and H. Song, 2006: Evidence of deceleration of atmospheric vertical overturning circulation over the tropical Pacific. *Geophys. Res. Lett.*, **33**, L12701, doi: 10.1029/2006GL025942.